QUANTIFYING MOSQUITO SPERM MOTILITY PATTERNS: HIGH SPEED ACQUISITION AND ANALYSISOF FLAGELLAR WAVEFORMS

By

Sueann Lin

A capstone project submitted for
Graduation with University Honors

Jun 4, 2020

University Honors
University of California, Riverside

APPROVED

_____
Dr.Richard Cardullo
Department of Department of Biology

_____
Dr. Richard Cardullo, Howard H Hays Jr. Chair, University Honors

Abstract

Mosquitoes transmit many enzootic diseases that infect humans and other animals. The overall goal of this study is to ultimately identify methods to control mosquito populations by interfering with their reproduction, possibly through genetic manipulation of the male reproductive tract. Previous research has shown, in the common southern house mosquito, Culex quinquefasciatus, that the sperm flagellum progresses through three distinguishable waveforms following activation by a serine protease from the accessory glands. The initial wave form, A, is characterized by a low amplitude, long waveform pattern that leads to progressive motility at low speed. Within two minutes, a double waveform with a superimposed waveform, B, is observed with detectably greater velocity. Finally, the mosquito sperm exhibits vigorous progressive motility at a velocity of ~100 μm/sec that is powered by a large amplitude, high beat frequency flagellar beat (waveform C). Although mosquito sperm velocities have been previously measured, no detailed studies on flagellar amplitude or beat frequency have been performed. In this study, I quantified these parameters using darkfield microscopy, high speed digital photography, and image processing. Using these parameters, I mathematically modeled the sperm flagellum using existing theories. Ultimately this quantitative information will be used to understand the relationship between flagellar beat patterns and previously identified signal transduction pathways that lead to sperm activation in mosquitoes.

Acknowledgements

I would like to express my great appreciation to my faculty member and primary investigator, Dr. Richard Cardullo, for his patient guidance and encouragement throughout my undergraduate career at the University of California, Riverside. He has been supportive not only with developing my capstone, but also with my academic courses. I also want to give thanks to Dr. Catherine Thaler who taught me a lot of lab technique and gave me valuable advice. Additionally, I would like to show my gratitude to Dr. Edward Platzer with the mosquitoes' colony maintenance. Lastly, I would like to thank Emily Harris, my fellow undergraduate laboratory member, for teaching me the dissection and other lab techniques.

Table of Contents

INTRODUCTION

I. Relevant Background – Mosquitoes as vectors of disease

Culex quinquefasciatus is the common southern household mosquito that is closely related to *Culex pipiens.* As a vector of disease, it transmits arbovirus West Nile (WNV) and St. Louis encephalitis (SLEV) causing worldwide illnesses in humans and other animals. In developing countries, the spread of disease by mosquitoes is a major concern due to lack of sanitary and sewage systems (Turell, 2012). In order to prevent outbreaks from these diseases, regulating mosquito population is a necessary step. Therefore, the research in this capstone project involved experiments that target mosquito reproduction, primarily on the sperm, to identify future methods to control mosquito populations.

II. Basic Sperm Architecture and Mechanisms of Movement

In mosquitoes, mature sperm in males are stored in the seminal vesicle and remain quiescent prior to activation and release into the female reproductive tract. A signaling cascade involving a trypsin-like protease that is released from male accessory glands activates the sperm resulting in the initiation of motility (Stephens et al., 2018). This sperm activation event also requires an influx of extracellular calcium through a presumed, yet to be identified, plasma membrane ion channel (Thaler et al., 2013). Following activation, the mosquito sperm flagellum goes through three successive changes of waveforms (A, B, and C; Figure 1) that ultimately leads to progressive motility of the sperm with increased amplitude, beat frequency, and velocity (Thaler et al., 2013).

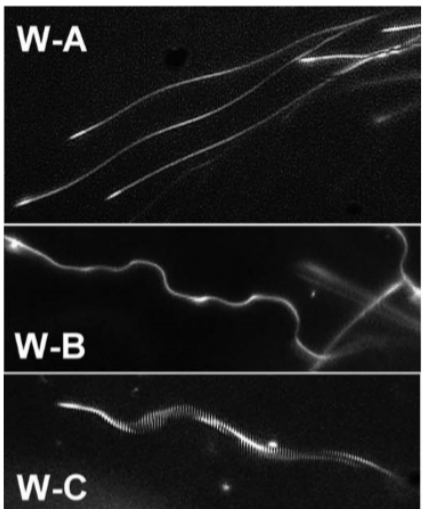

Figure 1. Progression of waveform A to C of *Culex quinquefasciatus* sperm.

Reprinted from "Waveform Generation Is Controlled by Phosphorylation and Swimming Detection Controlled by Ca^{2+} in Sperm from the Mosquito Culex quinquefasciatus" (Thaler et al… 2013).

The underlying mechanism for flagellar beating is well known and results from the sliding of doublet microtubules generated by the molecular motor, dynein, in the axoneme. The axoneme provides the supporting scaffold for the dynein and converts the energy from ATP hydrolysis to sliding and a flagellar oscillation (Pelle et al, 2009).

Unlike many eukaryotic sperm, like those from mammals, with an underlying "9+2" microtubule architecture in their axoneme, mosquito sperm possess a "9+9+2" pattern (Figure 2) with two concentric circles consisting of nine outer singlet accessory microtubules and nine doublet microtubules surrounding a pair in a central tube (Phillips, 1970).

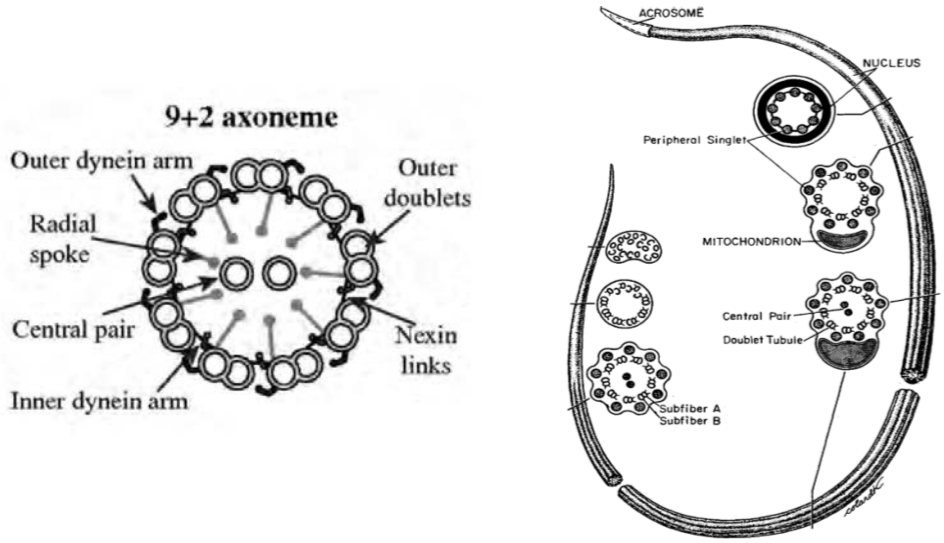

Figure 2. **Diagram of common "9+2" of mammalian sperm (Left).** *Reprinted from "mammalian sperm flagella and cilia" (Guan 2009).*
Diagram of "9+9+2" pattern in the axoneme of insect sperm (Right). *Reprinted from "Insect sperm: their structure and morphogenesis" (Phillips 1970).*

III. Flagellar structure as it relates to function: Flagellar morphology and the regulation of sperm motility

Sperm motility is greatly affected by its morphology. In multiple studies, it has been demonstrated that there is a tradeoff between sperm length and longevity (Werner and Simmons 2008). In mammalian sperm, there is a linear correlation between mitochondrial volume and flagellar length and this ultimately can be used to predict flagellar power output (P) and overall ATP hydrolysis rates in motile sperm (Cardullo and Baltz, 1991).

Understanding the underlying molecular mechanisms of sperm motility informs the flagellar behavior. The curvature of the flagellum controls active shearing the results from doublet sliding. When the curvature reaches a critical level, the sliding is locally switched OFF, while the opposite side of axoneme is switched ON (Brokaw 2009). This alternate switching leads to an oscillation of the flagellum which is characterized by wavelength parameters including wavelength, amplitude, and flagellar beat frequency.

IV. Environmental factors that affect flagellar motion

In addition to the action of dynein in the axoneme, sperm motility is also affected by environmental stimuli since the flagellum also effectively functions as a sensor. The sensors on the sperm surface orient the sperm toward the egg. In many studies, it has been shown that solution viscosity, Ca^{2+}, Mg^{2+}, and ATP concentration can greatly influence sperm movement. Increasing viscosity slows down the sperm because of increased drag. However, viscosity also leads to changes in the flagellar beat pattern, which alters both the bend angle and the beat frequency (Brokaw 1974). In the tunicate, *Ciona intestinalis*, as the viscosity of the solution increases, the sperm pattern changes from a planar to a helical wave (Brokaw 1996).

Calcium is a highly conserved second messenger in animals (Degner and Harrington, 2016). Mosquito sperm are highly affected by the concentration of Ca^{2+} in that higher calcium concentrations often leads to higher speed waveform. Interestingly, in the presence of a phosphodiesterase inhibitor that promotes overall phosphorylation in the cell, and when calcium is removed from the medium, mosquito sperm will swim backwards with the tail at the leading edge of movement. (Thaler et al., 2013)

V. Analyzing Flagellar Parameters using High Frame Rate Cameras

In this study, I designed experiments to quantify beat amplitude, beat frequency, flagellar curvature, initial velocity, and flagellar wavelength of mosquito sperm. These parameters are necessary to completely characterize mosquito sperm behavior in response to changing environmental conditions. In addition, accurate quantitative determinations of these parameters can be used to calculate the flagellar power output of the three distinct waveforms.

There are many approaches to measure sperm motility but, given the high rate of flagellar oscillations, acquisition speed and camera frame rate are critical to obtain reliable images over time. Previous studies on mosquito sperm motility used slower frame rate cameras with acquisition rates less than or equal to 30 frames per second (fps). For flagellar beat frequencies approaching or exceeding the frame rate of the camera, accurate determinations of flagellar beat frequencies are not possible. Our laboratory recently acquired a camera that can collect images of frame rates up to 500 fps making flagellar beat frequency determination possible. In addition, as an alternative to manually quantification, image processing allows for rapid and accurate determinations of flagellar parameters. SpermQ is a newly developed software package that has the ability to measure and analyze flagellar beat parameters using time-lapse image sequences filmed under dark-field microscopy (Hansen et al., 2018). The software incorporates different mathematical models to increase the accuracy of tracking sperm motility. The software detects the flagellar trace, and constructs normal lines, perpendicular to the sperm flagellum, along with a Gaussian curve to precisely determine flagellar location. In addition, the software also quantifies various head and flagellar parameters.

METHODS

Dissection of male seminal vesicles from mosquitoes

Mosquitoes were taken from an autogenous lab colony maintained by Professor Edward Platzer and rendered unconscious under an atmosphere of carbon dioxide. Male *Culex quinquefasciatus* were selected from the colony and placed individually in 1.25 ounce Solo™ cups with lids with holes for air and added sugar water for moisture and nutrients. Mosquitoes were euthanized with a cotton ball soaked in chloroform and the reproductive tract was dissected in 1X Phosphate-Buffered Saline (PBS) on a dissection slide. Seminal vesicles were obtained from the last segment of the mosquitoes and the exoskeleton and attached fat to the seminal vesicles was removed.

Preparation of slides

Seminal vesicles were placed on a microscope slide with insect Ringer solution (110 mM NaCl, 5 mM KCl, 0.5 mM $CaCl_2$, 1.2 mM MgCl2, 1.2 mM $MgSO_4$, 1.2 mM Na HCO_3, 2 mM KH_2PO_4, 2 mM Na_2 HPO_4, 1mM glucose, 20mM HEPES, pH 7.4) at room temperature. A cover slip was placed on top of the slide with single folded double-sided tapes in between to create a chamber with consistent depth of 152.4 µm. At times, an open chamber, consisting of a round well was used to observe sperm movement at a wider range of depth.

Darkfield and High Frame Rate Imaging

A darkfield condenser was used on an upright Nikon microscope to increase the contrast. Images were taken at 300 frame/sec or 100 frame/sec rate using either a 10X or 20X objective lens. Images were recorded using either a Pco.dimax or Edgertronic SC1 high frame rate camera.

Image Processing & Analysis

ImageJ (NIH) was used to calibrate the digital pixel distance value into microns. Images were reduced and cropped to focus on an ROI (region of interest) and decrease the time for processing. Images were prepared for analysis by adjusting the brightness and contrast (Fig. 3A & 3B), threshold, background, and signal-to-noise ratio. The processed images were then analyzed manually with trackmate on ImageJ to quantify the distance travelled by tracking the head (Fig. 3D). The measurement of body length was from head to tail, the wavelength was from one curve peak to another curve peak, and the amplitude was taken by the average of half the distance of peak to trough (Fig. 3C). The processed images were also analyzed via SpermQ, an image processing software package that quantifies sperm motility parameters. SpermQ traced the sperm head with the brightest intensity into points (Fig. 4) and reconstructed the flagellar trace with normal lines and a Gaussian curve (Fig 5).

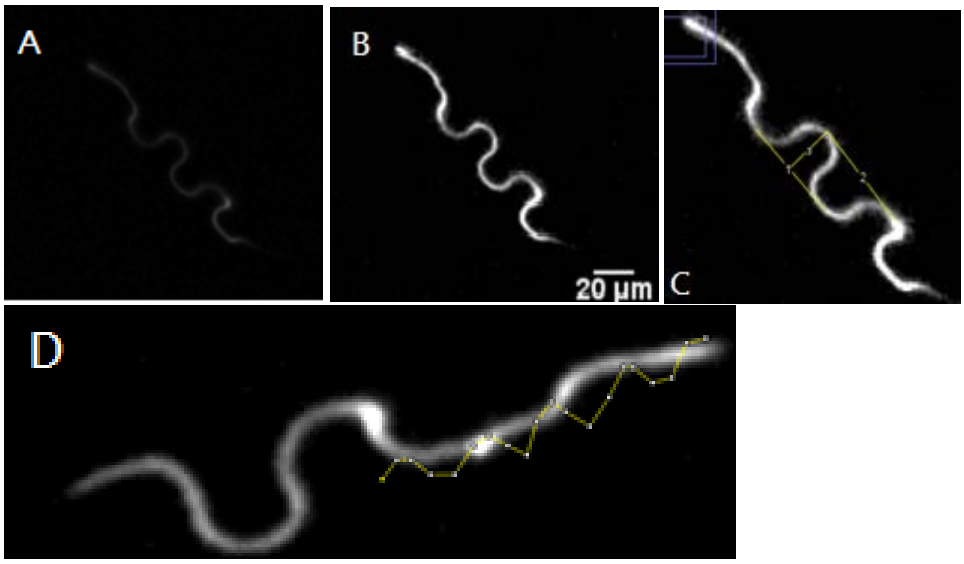

Figure 3. **Manually Measuring Motility Parameters**
A) Raw image of a single mosquito sperm. B) Processed image to enhance contrast and brightness. C) Two parallel yellow lines from one curve peak to another were used to measure the flagellar wavelengths. Similarly, the amplitude was calculated as half of the distance from the peak to the trough of the wave (nearly perpendicular to the 2 parallel yellow lines). D) The dots represent the sperm head at different frames or time, and the line connecting the dots denotes the distance travelled.

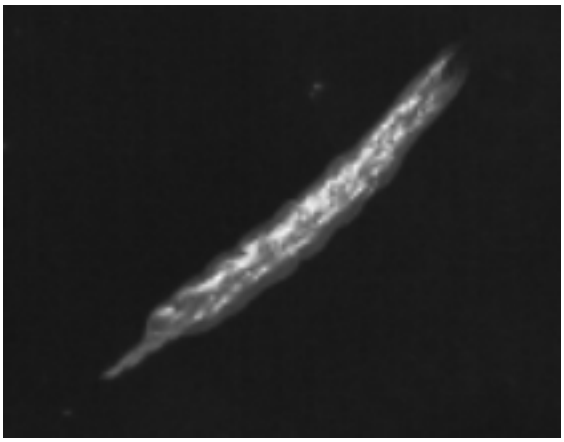

Figure 4. **Using SpermQ to Track Mosquito Sperm Head Movements**
The head with the brightest intensity in each time frame was tracked, tracing the distance travelled.

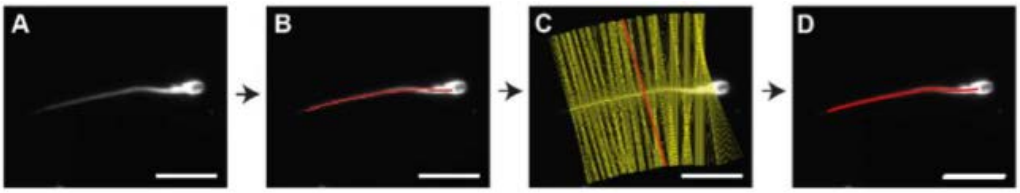

Figure 5. Steps Used to Reconstruct the Flagellar Trace
A) sperm was skeletonized B) flagellum (red) was roughly traced C) normal lines (yellow) were constructed by using the tangential vectors D) Gaussian curve was used to obtain precise flagellar trace.

Reprinted from "Waveform Generation Is controlled SpermQ A Simple Analysis Software to Comprehensively Study Flagellar Beating and Sperm Steering" (Hansen et al 2018).

RESULTS

From the high frame rate recording of sperm motility, waveform A that was characterized by a low amplitude waveform and slow beat frequency was readily distinguished from waveforms B and C. After activation, both the amplitude and the speed of the sperm increased. The sperm swam with a helical trajectory with their flagellum going in (Fig. 6A) and out (Fig. 6B) of focus. Unlike previous studies using a camera with lower spatial and temporal resolution (Thaler et al., 2013), it was difficult to distinguish waveform B and C, except sperm that exhibited Waveform B followed a linear trajectory while sperm that exhibited waveform C had higher velocities and moved along a curve (Fig. 7). When mosquito sperm were placed in deeper wells or placed into a lidless-well (i.e., without a coverslip), they would go out of focus more frequently indicating free swimming behavior.

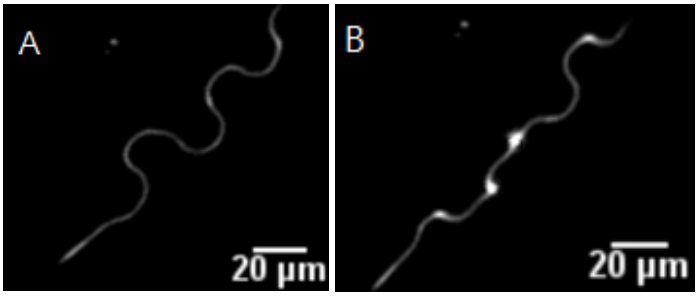

Figure 6. Mosquito Sperm Exhibit Helical Swimming Behavior
Both images were obtained from the same sperm of a single recording. A) When the entire flagellum was in the same plane, the wave pattern displayed clear peaks and troughs. B) As the sperm moved forward the flagellum was in and out of focus indicating that the sperm was swimming in a helical pattern.

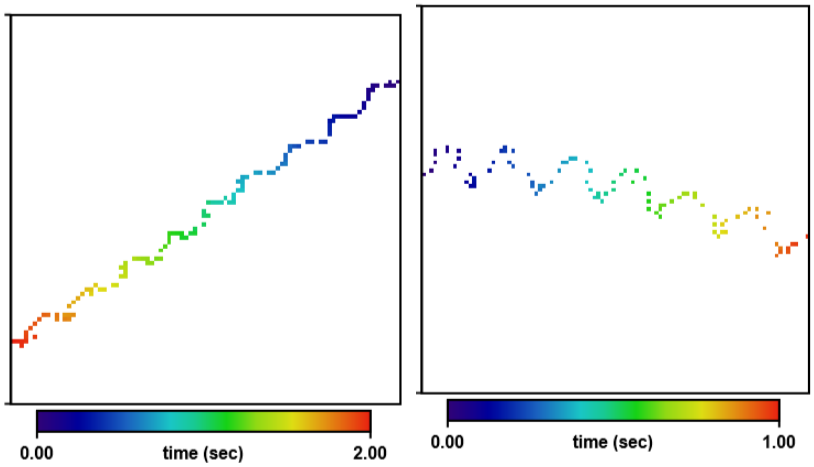

Figure 7. **Flagellar Waveforms B and C are Markedly Different**
This diagram shows the head position of sperm in different time frames. Waveform B would move in a straighter path (Left) while Waveform C would move in a more curved path (Right).

Based on several measurements of waveforms B and C, the average of the flagellar amplitude was 7.72 µm with a standard deviation of 0.96 µm (Table 1). The beat frequency measured manually and by SpermQ (Fig. 8) were relatively close to one another. Both methods revealed an average of approximately 4 beats per second (Table 1). The average sperm length measured manually was 118.09 $\pm$ 15.07 µm (Table 2) whereas SpermQ yielded a consistently larger value longer measurement of 143.72 $\pm$ 15.33 µm (Fig. 7). The average wavelength, measure manually, was around 38.82±8.87 µm (Table 2).

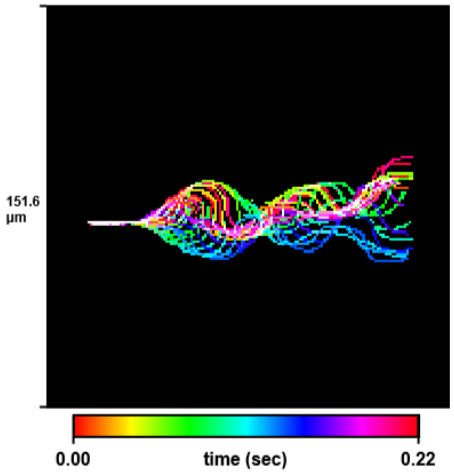

Figure 8. **Flagellar Waveform Overlays From One Sperm Beat Cycle**
This image combined sperm waveforms at different time or frames. The red to violet-red bar displays the timeline, with one beat cycle equaling 0.22 sec corresponding to a beat frequency of 4.55 beats/sec. On the left-hand side of the diagram, the length of this sperm was calculated as 151.6 µm.

The velocities differed based on whether they were manually determined or calculated by SpermQ. When sperm motility was tracked by hand frame-by-frame, the average velocity was 86.7 $\pm$ 34.4 µm/sec. In contrast, when the velocity was calculated by SpermQ, it had an average value of the velocity was 165.9 µm/sec $\pm$ 58.1 µm/sec which was nearly double that calculated manually (Table 3).

Aside from these measurements of sperm motility parameters in insect Ringer, motility patterns were also observed under different conditions. When okadaic acid was added and calcium was removed from the extracellular environment using a calcium chelator, the sperm began to move backward with same waveform but with the tail leading the sperm. When cyanide, an electron transport inhibitor was added to the insect Ringer, most sperm moved initially, but would stop progressive motility even though the flagellum still exhibited a beat pattern.

Trials	Amplitude (μm)	Manually Calculated Beat Frequency (beats/sec)	SpermQ Frequency (beats/sec)
1	6.96	2	2
2	7.12	6	6
3	8.02	4	4
4	7.01	5	5
5	6.83	6	6
6	8.85	5	5
7	9.71	4.5	4
8	7.33	4	4
9	7.70	2.5	2
10	6.86	2	2
11	8.70	3.5	2.7
12	8.05	4.5	4.5
Average + Standard Deviation	**7.72±0.96**	**4.13±1.33**	**3.93±1.47**

Table 1. Amplitude and Beat Frequency

The amplitude was the average measurement of the half distance between the peak and trough of the flagellar waveform. The beat frequency was counted both manually and by using SpermQ to determine the number of oscillation cycles per second.

Trials	Manually Calculated Sperm length (µm)	SpermQ Sperm length (µm)	Manually Calculated Wavelength (µm)
1	117.6	140.7	36.6
2	126.9	155.3	44.1
3	124.7	162.6	42.4
4	138.2	162.6	64.1
5	111.1	132.4	34.5
6	121.8	145.2	37.4
7	110.3	140.7	32.9
8	88.5	117.8	37.3
9	100.8	121.5	29.3
10	107.4	133.4	36.6
11	136.1	160.8	35.5
12	133.5	151.6	35.1
Average + Standard Deviation	**118.09±15.07**	**143.72±15.44**	**38.82±8.87**

Table 2. Measurements of Overall Sperm Length and Wavelength

The sperm length was measured from head to tail and the sperm length measured by SpermQ was taken through precise traces of the flagellum by constructing normal lines with tangential vectors. The wavelength was measured from one peak/trough of the flagellum to the second peak/trough of the flagellum.

Trials	Manually Calculated velocity (μm/sec)	SpermQ velocity (μm/sec)
1	43.0	74.7
2	156.75	183.7
3	95.0	294.9
4	98.8	170.2
5	104.0	130.9
6	91.1	195.1
7	128.2	157.9
8	99.0	163.8
9	49.1	106.0
10	59.8	140.0
11	55.2	180.4
12	60.4	91.4
Average + Standard Deviation	**86.7 ± 34.4**	**165.9 ± 58.1**

Table 3. Determinations of Sperm Velocity

Velocity was determined via tracking the sperm head. The left column shows the data of the velocity measured manually and the right column shows the data of the velocity measured using the SpermQ software.

DISCUSSION

From these experiments, different parameters of mosquito sperm motility were measured. SpermQ had a more accurate and longer measurement on the sperm length than could be determined manually, because it traced the flagellum clearly with mathematical models that took all parts of the curve into account rather than estimate the length of the flagellum with straight line segments. The average of the beat frequency was consistent at approximately 4 beats/sec.Using both the length of the flagellum and the beat frequency, the power (P) production can be calculated (equation 1; Dresder and Katz 1981). The mean of the dimensionless number ($p = 0.5$), water viscosity ($\eta = 0.01$ poise) at 20 ˚ C, beat frequency ($f = 3.93\ sec^{-1}$), and length of the flagellum ($L = 1.44x10^{-2}cm$) were plugged into the equation to yield a power output of 2.3 $x10^{-7}$ ergs/sec in the mosquito sperm (equation 2). The power output of the mosquito is around 10% of the sperm power output of 2.6 $x10^{-7}$ ergs/sec for rat sperm (Cardullo and Baltz 1991). The reason that the power output in mosquito sperm is significantly lower than a rat sperm might be the absence of functional mitochondria in insect sperm resulting in lower beat frequencies if ATP is limiting. In these calculations, the hydrodynamic power output at a given solution viscosity is proportional to the square of the beat frequency and the third power of the length of the flagellum:

$$P = p\eta f^2 L_f^3 \quad (1)$$

$$P = (0.5)(.01\ poise)(3.93\ sec^{-1})(1.44x10^{-2}cm)^3 = 2.3\ x10^{-7}\ ergs/sec \quad (2)$$

This equation provides a crude estimation of the power output. Slender Body Theory, which is more sophisticated, uses the velocity and amplitude that generate flow fields into account (Johnson and Brokaw 1979). Nevertheless, the accuracy for the velocity and

amplitude measurement were obscured. It was difficult to precisely track the head by only focusing on the high intensity center mass in head, because the helical beating pattern of the flagellum would cause the tail to move in and out of focus creating as high intensity brightness as the head. The problem was solved by tracking not only the high intensity head region but also the direction of the sperm movement. Nevertheless, there was a substantial difference in the results of the measurements of velocity between manual tracking and SpermQ. The expected agreement between the two methods could not be found. Either the population of the data was not sufficient or there might be an error in either the manual tracking or the SpermQ method. In addition, the sperm flagellar amplitude was difficult to obtain manually due to the nature of the helical swimming pattern of free swimming mosquito sperm.

Besides these measurements on sperm motility parameters, there were a few interesting outcomes when either the physical or chemical environment were changed. When the sperm was placed in a lidless microscopic slide with a deeper depth, the sperm tended to swim in and out of focus, meaning they were swimming up and down rather than the more lateral swimming behavior in a constructed chamber (i.e., slide and a coverslip). Additionally, when calcium was removed and okadaic acid was added, the sperm would move backward instead (Thaler et al.,, 2013). Furthermore, when cyanide was added, the sperm's motility was affected. The inhibition in sperm movement raised the question concerning the energy source for sperm motility. Cyanide inhibits the mitochondrial electron transport chain by inhibiting cytochrome C oxidase. Insect sperm are thought to not possess functional mitochondria, so the addition of cyanide stopping the sperm movement means either that this contention is the incorrect, or a stored energy is maintained within the sperm until it can be mobilized by the protease that is necessary for sperm activation.

Overall, the sperm motility parameters gave an initial, albeit crude, estimate of the flagellar power output. Nevertheless, there was no discernible difference between waveform B and C. A logical next step would be to improve the measurements on amplitude and wavelength that would yield more accurate determinations of power output using the more sophisticated slender body model, so that differences between waveform B and C might be observed. Another future direction would be to identify the energy source for mosquito sperm motility, as no additional glucose was added during the experiments, but the sperm continue to move. It would be interesting to understand where and how the mosquito sperm get its energy that is needed for the activation and maintenance of sperm motility in the female reproductive tract of mosquitoes..

REFERENCES

Brokaw, C. J. (2009). Thinking about flagellar oscillation. *Cell Motil Cytoskeleton*, 66(8), 425-436. doi:10.1002/cm.20313

Brokaw, C. J. (1996). Microtubule sliding, bend initiation, and bend propagation parameters of Ciona sperm flagella altered by viscous load. *Cell Motil Cytoskeleton*, 33(1), 6-21. doi:10.1002/(SICI)1097-0169(1996)33:1<6::AID-CM2>3.0.CO;2-C

Cardullo, R. A., and Baltz, J. M. (1991). Metabolic regulation in mammalian sperm: Mitochondrial volume determines sperm length and flagellar beat frequency. *Cell Motil. Cytoskeleton*, 19, 180-188. doi:10.1002/cm.970190306

Degner, E. C., Harrington, L. C. (2016). A mosquito sperm's journey from male ejaculate to egg: Mechanisms, molecules, and methods for exploration. *Mol Reprod Dev.*, 83(10),897-911. doi:10.1002/mrd.22653

Dresdner, R. D., and Katz, D. F. (1981) Relationships of Mammalian Sperm Motility and Morphology to Hydrodynamic Aspects of Cell Function, *Biology of Reproduction*, 25(5), 920–930, doi: 10.1095/biolreprod25.5.920

Guan, J. (2009). Mammalian sperm flagella and cilia. Masters Thesis, Karolinska Institute, Stockholm, Sweden.

Hansen, J. N., Rassmann, S., Jikeli, J. F., Wachten, D. (2018). SpermQ⁻A Simple Analysis Software to Comprehensively Study Flagellar Beating and Sperm Steering. *Cells*, 8(1),10. doi:10.3390/cells8010010

Johnson, R. E., Brokaw, C. J. (1975). Flagellar hydrodynamics. A comparison between resistive-force theory and slender-body theory. *Biophys J*, 25(1),113-127. doi:10.1016/S0006-3495(79)85281-9

Pelle, D. W., Brokaw, C. J., Lesich, K. A., Lindemann, C. B. (2009). Mechanical properties of the passive sea urchin sperm flagellum. *Cell Motil Cytoskeleton*, 66(9),721-735. doi:10.1002/cm.20401

Phillips, D. M. (1970). Insect sperm: their structure and morphogenesis. *J Cell Biol*, 44(2),243-277. doi:10.1083/jcb.44.2.243

Stephens, K., Cardullo, R. A., Thaler, C.D. (2018) *Culex pipiens* sperm motility is initiated by a trypsin-like protease from male accessory glands. *Mol Reprod* , 85, 440– 448. doi: 10.1002/mrd.22980

Thaler C. D., Miyata H., Haimo L. T., Cardullo R. A. (2013). Waveform generation is controlled by phosphorylation and swimming direction is controlled by Ca2+ in sperm from the mosquito Culex quinquefasciatus. *Biol Reprod*, 89(6),135. doi:10.1095/biolreprod.113.109488

Turell, Michael J. (2012). Members of the Culex pipiens Complex as Vectors of Viruses, *Journal of the American Mosquito Control Association*, 28(4s), 123-126.

Werner M., Simmons L. W. (2008). Insect sperm motility. *Biol Rev Camb Philos Soc*, 83(2),191-208. doi:10.1111/j.1469-185X.2008.00039x